Design and Computational Modeling of a Leg-Wheel Transformable Mechanism with Decoupled Kinematics

José F. Flores, Héctor A. Moreno, Isela G. Carrera, and José Luis Ordoñez-Avila, *Member, IEEE*

***Abstract*—This paper presents the design of a novel leg-wheel transformable mechanism. The purpose of this mechanism is to combine the efficiency of wheeled locomotion with the ability of the legs to traverse difficult terrain. The mechanism has two degrees of freedom with decoupled kinematics. The decoupled kinematics of the mechanism allows the rotation and extension/flexion motions to be controlled independently by a pair of actuators, which provides some advantages. In this work, the direct kinematics of the mechanism is solved analytically. On the other hand, due to the complexity of the inverse kinematics, two different numerical methods were evaluated for solving this problem. A model based on neural networks was successfully implemented in a physical prototype to generate the trajectory of a gait cycle in the leg mode of the mechanism. The proposed design enables seamless transitions between wheeled and legged locomotion, enhancing versatility across terrains and contributing to SDG 3 in assistive mobility, as well as SDGs 8 and 9 through advances in agricultural robotics.**

Link to graphical and video abstracts, and to code: https://latamt.ieeer9.org/index.php/transactions/article/view/9828

***Index Terms*—Transformable mechanisms, kinematics, neural networks, mobile robotics.**

I. Introduction

ADVANCES in artificial intelligence and the continuous development of new hardware components with improved performance are significantly driving the progress of mobile robotics, and it is foreseeable that this technology will be adopted in various areas of human activity in the near future. In recent years, the design of multimodal locomotion systems has garnered significant interest among researchers. By integrating various elements like wheels, tracks, and legs into a single vehicle, these systems can dynamically switch to the most appropriate locomotion mode depending on the terrain [1]. Among the most common locomotion methods in terrestrial environments are wheels and legs, each providing distinct benefits. Multimodal systems that combine both approaches can effectively utilize these advantages. Wheeled locomotion is particularly efficient on flat surfaces, often surpassing legged systems in speed and energy consumption on smooth terrain [2]. Conversely, legged systems excel in unstructured environments, where their superior ability to navigate complex and uneven terrains ensures enhanced maneuverability. This flexibility makes multimodal systems particularly well-suited for diverse and challenging operational conditions.

The locomotion systems based on wheels and legs can be classified in:

1) Platforms with legs and wheels. These are systems that integrate legs and wheels in the same platform, allowing independent or combined operation to adapt to different terrains. In this scheme, the robot uses wheels to move, retracting the legs until an obstacle prevents the wheels from moving forward, at which point the legs are deployed to overcome the obstacle [3], [4].
2) Wheeled legs. In these systems, wheels are mounted at the ends of mechanical limbs. This configuration allows the position of the wheels to be adjusted relative to the robot's center of mass, enabling the vehicle to navigate obstacles while maintaining stability. These systems can perform leg-like motions, such as walking, climbing or jumping, offering enhanced mobility on uneven surfaces. [5], [6].
3) Legged wheels. A legged wheel is a symmetrical body with multiple limbs, rotated by an actuator mounted in the vehicle's chassis. This design allows vehicles to traverse rough terrain, such as gravel and rubble, enhance traction on slippery surfaces like sand, mud, and snow, and even climb stairs [7]–[9] .
4) Transformable legged wheels. These are mechanisms with multiple limbs symmetrically distributed around the rotation axis of the wheel. Therefore they are legged wheels that can change their geometry, and in some designs can transform into circular wheels. In this way, these mechanism have the capacity to adapt to varying terrain conditions. [10]–[12].
5) Leg-Wheel transformable mechanisms. These devices are mechanisms that can adopt a circular shape like that of a wheel, and when extended can perform movements like those of a leg. The purpose of these mechanisms is to provide the advantages of both locomotion systems. [13], [14].

There are few previous publications on transformable leg-wheel mechanisms [13]–[17]. Tadakuma et al. [13] introduced

The associate editor coordinating the review of this manuscript and approving it for publication was Javier Moreno-Valenzuela (*Corresponding author: Jose Ordoñez*).

J. F. Flores, H. A. Moreno, and I. G. Carrera are with the Facultad de Ingeniería Mecánica y Eléctrica, Universidad Autónoma de Coahuila, Monclova, México (e-mails: fidencio.flores@uadec.edu.mx, h_moreno@uadec.edu.mx, and iselacarrera@uadec.edu.mx).

Jose Ordoñez-Avila is with Facultad de Ingeniería, Universidad Tecnológica Centroamericana, San Pedro Sula, Honduras (e-mail: jlordonez@unitec.edu).

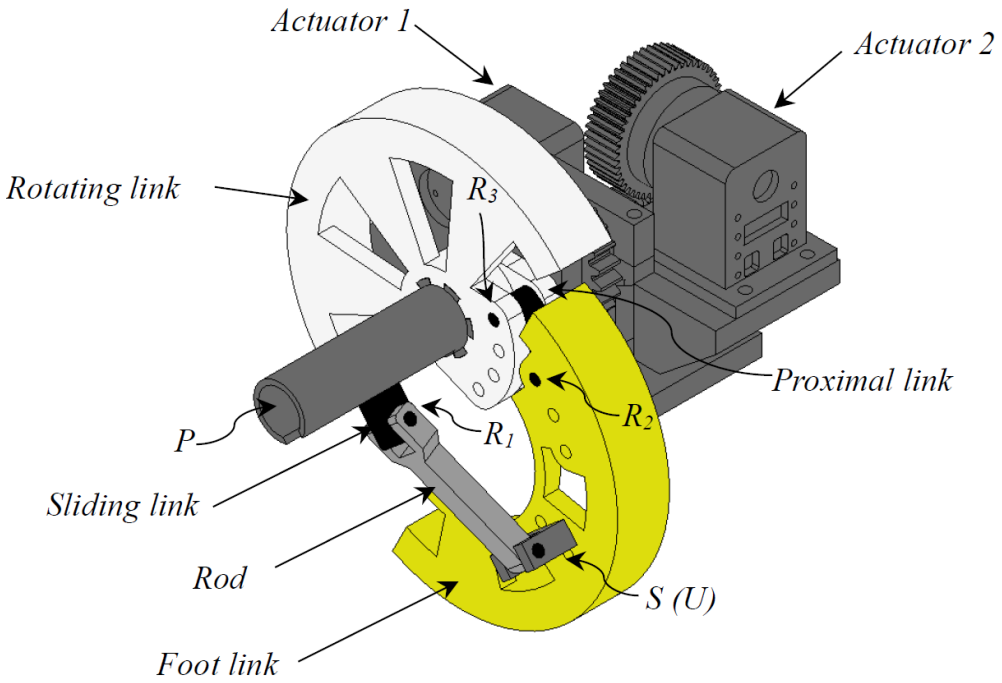

Fig. 1. Topology of the leg-wheel transformable mechanism. Actuator 1 controls the movement of the Rotating link, and Actuator 2 controls the position of the Sliding link through a rack and pinion transmission.

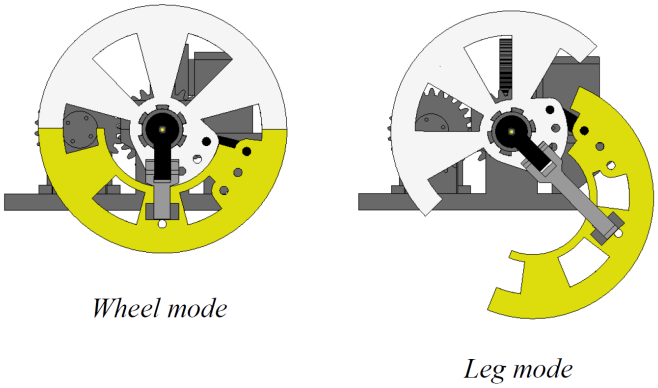

Fig. 2. Wheel and leg modes of the transformable mechanism.

a transformable wheel utilizing a serial mechanism of three degrees of freedom. When extended, this mechanism converts into a leg, enabling the robot to perform walking motions. Lin and Shen [14] proposed a wheel design that transforms into a C-shaped leg by rotating the two halves of the wheel around an axis perpendicular to its rotation axis. An actuator embedded in the wheel rim facilitates this transformation. Chen et al. [15] developed a module with two degrees of freedom, featuring an 11-link mechanism that enables quick transitions between wheel and leg modes, allowing for wheel-to-leap behavior. In [16] Xue et al. presents a leg-wheel transformable mechanism based on the 5 bar mechanism. Moreno [17] presented the LW.Transmech, a seven-link mechanism with two degrees of freedom, capable of transforming a leg into a circular traction device, providing effective contact with the ground surface.

The proposed design allows for seamless switching between wheeled and legged locomotion, improving versatility when traveling over different terrains. The applicability of these wheels is evident in SDG 3, through their use in assistive technologies for people with disabilities [18], and in SDGs 8 and 9, by contributing to the advancement of mobile robot technologies for monitoring agricultural farms [19].

This work is divided into several sections, which are described to facilitate understanding. Section II describes the design of the transformable mechanism, showing its components, degrees of freedom, and advantages over other mechanisms. Section III develops direct kinematics using analytical methods, and to solve inverse kinematics, two different methods are evaluated: Newton-Raphson and Neural Networks. Section IV shows the results of the neural network model tests for inverse kinematics. Finally, the conclusions summarize the findings, highlighting the mechanism's potential applications and future research directions.

II. Leg-Wheel Transformable Mechanism

Fig. 1 shows the components of the mechanism. Fig. 2 shows the transformable mechanism in its wheel and leg modes. The mechanism includes a rotating link that is connected to the chassis by a rotational joint. The rotating link is connected to a proximal link by means of the rotational joint R_3. At the other end the proximal link is connected to the foot link by means of the rotational joint R_2. The foot link is connected to the rod by means of the spherical joint S. When the plane of motion of the foot link is orthogonal to the axis of rotation of the wheel the joint S can be substituted by a universal joint U. At the other end the rod is connected to a

sliding link by means of the rotational R_1. Finally the sliding link is connected to the rotating link by means of the prismatic joint[1] P.

The number of degrees of freedom of the mechanism can be obtained by the Grübler Kutzbach criterion:

$$m = \lambda(n - j - 1) + \sum j_i \tag{1}$$

where m is the number of degrees of freedom (dof), λ is the number of degrees of freedom of the space in which the mechanism moves, n is the number of links, j is the number of joints. The sum of the degrees of freedom of the joints is calculated in the following way:

$$\sum j_i = j_1 + 2j_2 + 3j_3 + \cdots + 6j_6 \tag{2}$$

where j_i is the number of joints with i degrees of freedom. For the mechanism we have that $\lambda = 6$, $n = 6$, $j = 6$, $j_1 = 5$, $j_2 = 0$, $j_3 = 1$, and therefore $m = 2$ dof. The mechanism is driven by two motors. Actuator 1 is coupled to the rotating link, so that it controls its rotation. On the other hand, the prismatic joint P is actuated by a second actuator. In the prototype presented in Fig. 2, Actuator 2 moves the sliding link linearly through a rack and pinion gear. Since the sliding link rotates (with the movement of the rotating link), this link is connected to the rack through a rotational joint. Linear motion of the sliding link can be provided by a linear actuator mounted on the robot chassis, or by motion provided by a power transmission mechanism of another kind.

This device is characterized by the fact that both actuators are placed on the chassis of the vehicle, and are not placed inside the structure of the mechanism, as it is in the case of [13], [14]. Placing motors inside the structure of the mechanism implies that the mass and volume of the actuators will be included in the structure of the mechanism, making it heavier and larger. Moreover, since the wheel rotates more than 360°, complex wiring is required to transmit electrical power and control signals to the actuators inside the structure.

The presented device has the advantage, with respect to the designs of [15]–[17], that the rotation and extension movements of the leg are decoupled, allowing that in wheel mode only the Actuator 1 works, and the movement of the Actuator 2 is not required. On the other hand, the previous mentioned mechanisms require perfect coordination of the two rotational actuators to achieve the circular shape in wheel mode, any variation in the speeds of the motors will cause that the circular shape is lost to some extent.

An interesting application of the presented mechanism is the construction of a vehicle with multiple legs of one degree of freedom. This type of legs consists of a limb made of one piece that is connected to a rotational motor and that is permanently rotating during walking. An example of a vehicle with one degree of freedom legs is the RHex robot [20], which has proven to be effective for traversing various types of difficult terrain. RHex is a hexapod robot that walks using three legs alternately and whose gait is inspired by the biomechanics of arthropod locomotion. Using the transformable mechanism presented in this work, this type of legged vehicle could be transformed in a wheeled vehicle. Thanks to the fact that the rotation and extension movements of the leg are decoupled, the transformation of all the legs can be achieved with a single actuator that provides, through a transmission mechanism, the translational movement to all the prismatic joints of the leg-wheel transformable modules.

[1]The implementation of the mechanism shown in fig. 1 was designed for explanatory purposes, so that the kinematic chain would be clearly exposed and the operating principle made evident. In a practical vehicle application, the stroke of the prismatic joint would be contained within the vehicle structure, rather than extending outward beyond the wheel.

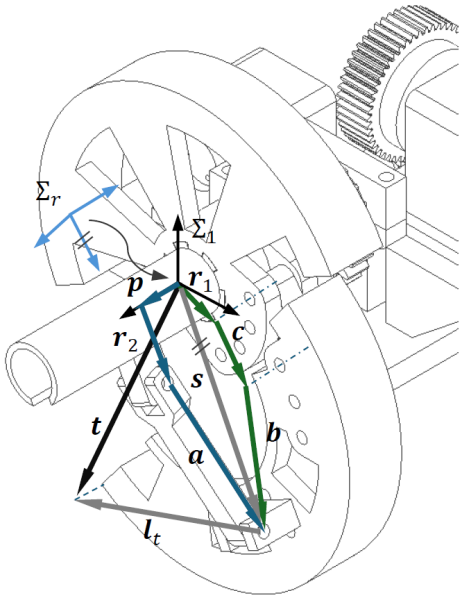

Fig. 3. Vectors used in the kinematic analysis of the transformable mechanism. The reference frame Σ_1 is fixed to the chassis, while the reference frame Σ_r moves with the rotating link; both frames share the same origin.

Although the mechanism has uncoupled kinematics, in order to perform walking patterns in leg mode it is necessary that the movements of the actuated joints be coordinated. The following section presents the kinematic modeling of the mechanism, which will allow the generation of trajectories in leg mode.

III. Modeling of the Mechanism

A. Forward Kinematics

The joint variables are defined by vector $\boldsymbol{q} = [q_r\,, q_p]^T$, where q_r is the joint variable associated with the rotational motor and q_p is associated with the linear actuator. The operational coordinates are defined by vector $\boldsymbol{t} = [t_x\,, t_y]^T$, where t_x and t_y are the coordinates of the tip of the foot link with respect to a reference frame located on the chassis of the vehicle.

Forward kinematic analysis consists in determining the position $\boldsymbol{t}$ given the values of the joint variabes $\boldsymbol{q}$. The position of the tip of the foot link is obtained with the following sum of vectors:

$$\boldsymbol{t} = \boldsymbol{r}_1 + \boldsymbol{b} + \boldsymbol{c} + \boldsymbol{l}_t \tag{3}$$

where $\boldsymbol{r}_1 = \langle R_{c1}, q_r\rangle$, $\boldsymbol{b} = \langle L_2, \theta_2\rangle$, $\boldsymbol{c} = \langle L_3, \theta_3\rangle$ and $\boldsymbol{l}_t = \langle L_t, \theta_2 + \vartheta\rangle$. R_{c1} is the distance from the wheel axis to the

joint R_3, L_2 is the distance from the joint R_2 to the joint U, L_3 is the lenght of the proximal link, and L_t is the distance from the joint U to the tip of the foot link. The angle ϑ defines the orientation of the line that joins the U joint with the tip of the foot link. Angles θ_2 and θ_3 can be determined from the follwing closed loop vector equation:

$$\boldsymbol{r}_1 + \boldsymbol{b} + \boldsymbol{c} = \boldsymbol{s} \tag{4}$$

where $\boldsymbol{s} = \langle S_p, q_r + \delta \rangle$ and δ is the angle between vectors $\boldsymbol{r}_1$ and $\boldsymbol{r}_2$. The solution of equation (4) gives:

$$\theta_2 = 2\tan^{-1}\left(\frac{Q_2 \pm \sqrt{Q_1^2 + Q_2^2 - P_1^2}}{P_1 + Q_1}\right) \tag{5}$$

and

$$\theta_3 = 2\tan^{-1}\left(\frac{Q_2 \pm \sqrt{Q_1^2 + Q_2^2 - P_2^2}}{P_2 + Q_1}\right) \tag{6}$$

where $Q_1 = S_p\cos(q_r+\delta) - R_{c1}\cos q_r$, $Q_2 = S_p\sin(q_r+\delta) - R_{c1}\sin q_r$, $P_1 = (S_p^2 + R_{c1}^2 - 2S_pR_{c1}\cos\delta + L_2^2 - L_3^2)/2L_2$ and $P_2 = (S_p^2 + R_{c1}^2 - 2S_pR_{c1}\cos\delta + L_3^2 - L_2^2)/2L_3$. The value of S_p is determined by solving the following equation:

$$\boldsymbol{a} + \boldsymbol{r}_2 + \boldsymbol{p} = {}^r\boldsymbol{s} \tag{7}$$

where $\boldsymbol{a} = \langle L_1, \theta_1 \rangle$, $\boldsymbol{r}_2 = \langle R_{c2}, \pi/2 \rangle$, $\boldsymbol{p} = \langle q_p - l_p, \pi \rangle$ and ${}^r\boldsymbol{s} = \langle S_p, \pi/2 \rangle$. L_1 is the length of the connecting rod, R_{c2} is the distance from the wheel axis to the position of joint R_1, and l_p is the distance from the origin of the reference frame from which the value of variable q_p is measured. Vectors $\boldsymbol{a}$, $\boldsymbol{r}_2$, $\boldsymbol{p}$ and ${}^r\boldsymbol{s}$ are measured respect to reference frame Σ_r that is attached to the rotating link and is oriented in such a way that the motion of the rod is contained in the plane x_r-y_r. The values of S_p and θ_1 are given by:

$$S_p = R_{c2} \pm \sqrt{L_1^2 - (l_p - q_p)^2} \tag{8}$$

and

$$\theta_1 = \tan^{-1}\left(\pm\sqrt{\left(\frac{L_1}{l_p - q_p}\right)^2 - 1}\right) \tag{9}$$

On the other hand, the relationship beetween the joint velocities and the operational velocities is given by the following equation:

$$\dot{\boldsymbol{t}}_i = \mathbf{J}\dot{\boldsymbol{q}} \tag{10}$$

where the Jacobian matrix of the mechanism $\mathbf{J}$ can be computed with $\mathbf{J} = \mathbf{M}\mathbf{K}^{-1}\mathbf{L} + \mathbf{N}$. Matrices $\mathbf{K}$ and $\mathbf{L}$ are obtained by deriving (7) and relates the actuated joints velocities $\dot{\boldsymbol{q}}$ and the passive joint velocities $\boldsymbol{\nu} = \begin{bmatrix}\dot{\theta}_2 & \dot{\theta}_3\end{bmatrix}^T$ with

$$\mathbf{K}\boldsymbol{\nu} = \mathbf{L}\dot{\boldsymbol{q}}, \tag{11}$$

where $\mathbf{K} = \mathbf{E}\begin{bmatrix}\boldsymbol{b} & \boldsymbol{c}\end{bmatrix}$, $\mathbf{L} = \begin{bmatrix}\mathbf{E}(\boldsymbol{s} - \boldsymbol{r}_1) & \hat{\boldsymbol{s}}/\tan\theta_1\end{bmatrix}$, $\hat{\boldsymbol{s}} = \boldsymbol{s}/S_p$ and matrix $\mathbf{E}$ is:

$$\mathbf{E} = \begin{bmatrix}0 & -1\\ 1 & 0\end{bmatrix}$$

Matrices $\mathbf{M}$ and $\mathbf{N}$ relates operational velocities with joint velocities obtained by taking the derivative of (3) giving

$$\dot{\boldsymbol{t}}_i = \mathbf{M}\boldsymbol{\nu} + \mathbf{N}\dot{\boldsymbol{q}}, \tag{12}$$

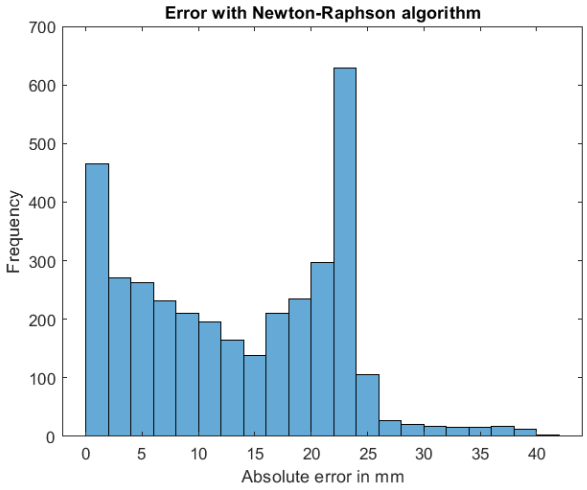

Fig. 4. Frequency histogram of the absolute errors for the Newton-Raphson method.

and $\mathbf{M} = \mathbf{E}\begin{bmatrix}(\boldsymbol{b} + \boldsymbol{l}_t) & \boldsymbol{c}\end{bmatrix}$ and $\mathbf{N} = \begin{bmatrix}\mathbf{E}\boldsymbol{r}_1 & \mathbf{0}\end{bmatrix}$. Jacobian matrix $\mathbf{J}$ will be used in the next section to solve the inverse kinematics using the Newton-Raphson method.

B. Inverse Kinematics

Solving the inverse kinematics of the mechanism involves solving a system of 6 transcendental equations, these are the equations (3), (4) and (7). Attempts to solve the problem analytically led to a system of two quadratic equations with two unknowns, whose numerical solution offers 8 possible solutions. Due to the difficulty of solving inverse kinematics in analytical form, we next evaluate two different numerical methods to solve this problem.

1) Newton-Raphson Method: The Newton-Raphson method is widely employed to solve nonlinear equations when an analytical solution is not feasible. Its primary advantage lies in its ability to provide approximate solutions to complex problems through an iterative process that utilizes the Jacobian matrix [21]. In this algorithm, given an initial guess of the joint variables $\boldsymbol{q}_i$ a vector $\boldsymbol{t}_i$ is computed, and then the difference between $\boldsymbol{t}_i$ and the value for which the inverse kinematics is to be solved, i.e. $\boldsymbol{t}_d$, is computed. This difference, $\Delta\boldsymbol{t} = \boldsymbol{t}_i - \boldsymbol{t}_d$, is used to compute the next estimate of the joint variables with $\boldsymbol{q}_{i+1} = \boldsymbol{q}_i + \mathbf{J}^{-1}\Delta\boldsymbol{t}$. If the difference between $\boldsymbol{q}_i$ and $\boldsymbol{q}_{i+1}$ is less than a given error, in this case $\|\boldsymbol{q}_{i+1} - \boldsymbol{q}_i\| < 0.005$, the loop stops and the solution, $\boldsymbol{q}_s$, of the inverse kinematics for $\boldsymbol{t}_d$ has been found. If not, the procedure is repeated. After 500 iterations the method is considered to have found no solution.

To evaluate the performance of this method, a set containing 10000 ordered pairs of $\boldsymbol{q}$ and $\boldsymbol{t}$ was created using the direct kinematics. For this dataset, the algorithm only converges for 35.6% of the points. In Fig. 4 the distribution of errors is shown. These absolute errors were calculated as the differences $AE = \|\boldsymbol{t}_d - \boldsymbol{t}_s\|$ between the correct values of $\boldsymbol{t}_d$ and the values of $\boldsymbol{t}_s$ obtained from those cases where the algorithm converges to a solution $\boldsymbol{q}_s$ given the convergence criterion previously described. For this mechanism, it was observed that

this method has a high dependence on the initial value of $\boldsymbol{q}$. These results show that this method is not suitable for on-line calculations to solve inverse kinematics. This would limit its use in reactive control architectures where rapid changes in the desired leg position may be required.

2) Modeling using Neural Networks : ANNs excel in their ability to approximate nonlinear functions without requiring knowledge of the system's internal structure [22]. This makes them a robust and flexible tool for modeling complex systems, such as inverse kinematics in robotics. A major advantage is that, once the neural network is trained, the kinematic calculations are direct and non-iterative, significantly reducing computational costs. However, a disadvantage is the need for a large amount of data to properly train the network, which can be a lengthy and costly process. Additionally, ANNs may generalize poorly if not adequately trained or if faced with situations outside the range of the training data.

The ANNs approach has been employed for solving the forward and inverse kinematics problems of different robotic mechanism. Among the proposed architectures, most models for function approximation are based on Radial Basis and multi layer perceptron networks [22]–[25]. In this work multi layer perceptron networks were used. A supervised learning approach was employed, where the network learns the mapping by observing the inputs and outputs derived from a dataset generated using the direct kinematics. An important factor to consider when designing a network is the number of outputs it will have. It could be considered that it would be appropriate to have a single network structure to solve the direct kinematics, having as input the two operational variables, and as output the two joint variables. From the results obtained in [24] and [25] some observations can be made:

- Using a single network for all the outputs requires larger hidden layers to achieve better precision
- Multiple networks (one per output) could improve precision with smaller hidden layers
- Computation time is affected by hidden layer size

Considering these observations, the ANNs structure was decided as follows: A neural network per output with number of hidden layers not greater than 3 and hidden layer size not greater than 30 neurons. The activation functions of the neurons are tangent-sigmoid. The dataset was divided in 70% training, 15% validation and 15% test. For this kinematic chain the optimal parameters and data set were obtained through experimentation where different combinations of training algorithms, parameters and data sets were employed arriving at the following combination:

- Levenberg-Marquardt training algorithm
- 3000 points data set
- 1 e^{-7} error goal
- 10000 epochs
- 500 validation checks

The performance of each network was tested using the same dataset employed to test the Newton-Raphson algorithm. The mean absolute errors (MAEs) and the maximum absolute errors (MaxAEs) were considered as indexes to measure the performance of the neural networks, additionally the relative amount of errors greater than 0.1 mm was considered. Table I presents the results of the 6 architectures that displayed the best performance. Since the MAEs of these networks was below 1 mm the distribution of errors between 0.1 mm and 1 mm was also a subject of interest to determine the best performance between all networks, this distribution can be observed in Fig. 5. Comparing all the results Net 1 was the one that had the best performance of all the ANNs. In this architecture, the network Q_r has three hidden layers, and the network Q_p has two hidden layers, each layer has 10 neurons. The obtained MAE was 0.0210 mm, the MaxAE was 0.3154 mm, and the percentage of errors greater than 0.1 mm was 1.3 %.The following section implements this architecture for experimental evaluation.

IV. Results of the Neural Network Model

To test the technical feasibility of the proposed kinematic structure and the neural network model, a prototype of the mechanism was developed. The neural network model was implemented on a Raspberry-Pi 4B. The model was programmed in Python and the integration of the control of the prototype was developed using the ROS libraries. The servomotors used are Dynamixel AX-12A from Robotix. The components of the mechanism were fabricated using 3D printing. In the wheel mode, the mechanisms has a radius of $R_w = 150$ mm. The geometric parameters of the links are $R_{c1} = 27.50$ mm, $R_{c2} = 23.75$ mm, $L_1 = 65.00$ mm, $L_2 = 62.43$ mm, $L_3 = 25.00$ mm, $\vartheta =$ -69.36 deg and $l_p = 59.46$ mm.

To implement a gait cycle a trajectory in the form of a semi-ellipse was chosen. The trajectory is executed in two parts, and each part is parameterized in time using a cycloidal function. Cycloidal functions have the characteristic that their initial and final velocities and accelerations are equal to zero, allowing a smooth transition between phases. The cycloidal function for this trajectory is given by the following expression:

$$f_{cyc} = \begin{cases} \dfrac{2t}{T} - \dfrac{1}{2\pi}\sin\left(\dfrac{4\pi t}{T}\right) & \text{if} \quad t < T/2 \\ \dfrac{2t-T}{T} - \dfrac{1}{2\pi}\sin\left(\dfrac{4\pi t - 2\pi T}{T}\right) & \text{if} \quad t \geq T/2 \end{cases} \tag{13}$$

where T is the period of time in which the trajectory is performed. The parametric equations of trajectory are the following:

$$\boldsymbol{t} = \begin{cases} \begin{bmatrix} C_x + A_g\cos(\pi - \pi f_{cyc}) \\ C_y + B_g\sin(\pi - \pi f_{cyc}) \end{bmatrix} & \text{if} \quad t < T/2 \\ \begin{bmatrix} C_x + A_g - 2A_g f_{cyc} \\ C_y \end{bmatrix} & \text{if} \quad t \geq T/2 \end{cases} \tag{14}$$

where C_x and C_y are the coordinates of the center of the semi-ellipse, and A_g and B_g are the lengths of the semi-axes.

For the implemented trajectory we have $C_x = 0$ mm, $C_y = -100$ mm, $A_g = 40$ mm and $B_g = 20$ mm. The trajectory is performed in $T = 2$ s, each phase of the gait cycle is performed in 1 s.

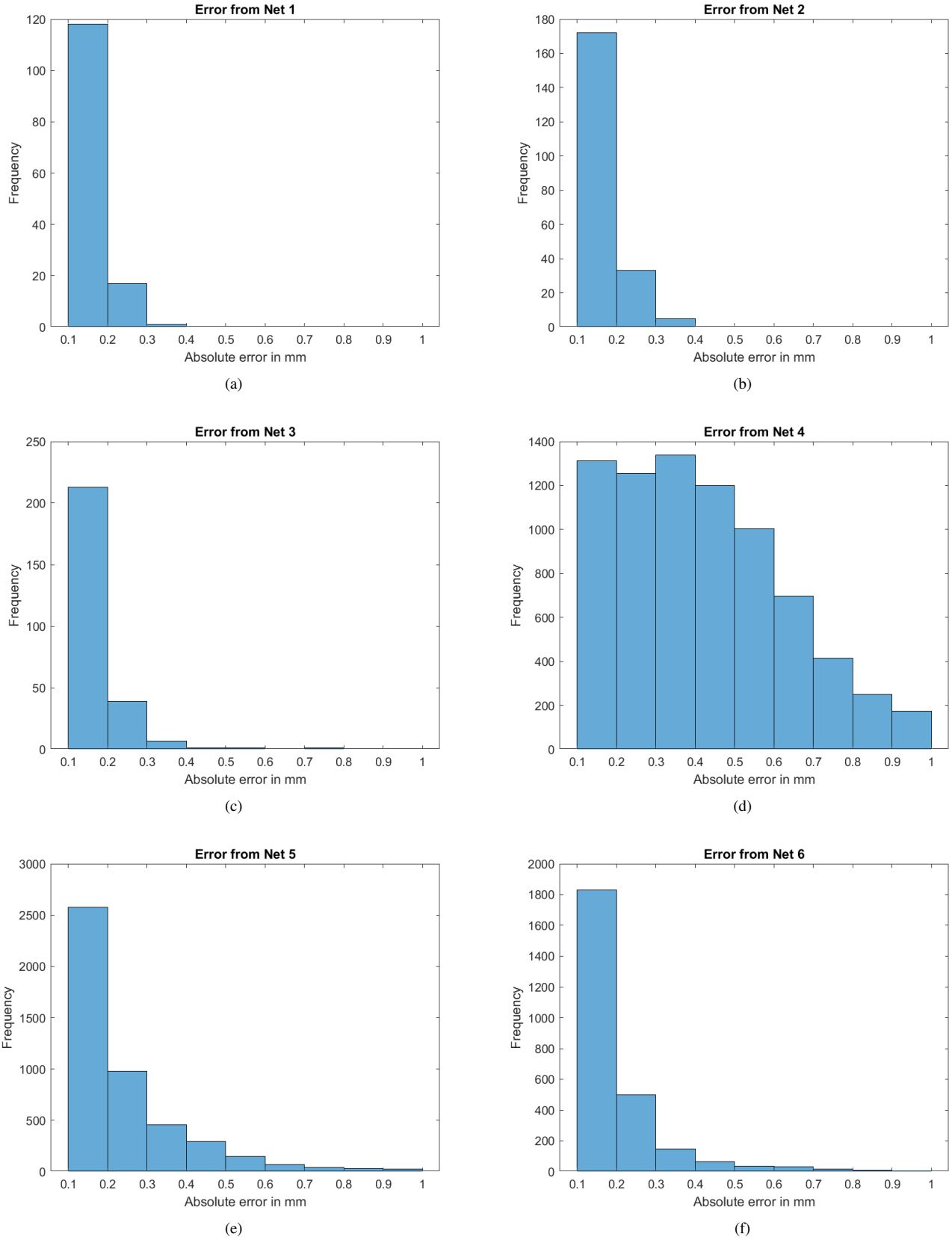

Fig. 5. Frequency histograms of the absolute errors for the selected structures of neural networks: a) Net 1, b) Net 2, c) Net 3, d) Net 4, e) Net 5 and f) Net 6.

TABLE I
PERFORMANCE AND CHARACTERISTICS OF THE SELECTED STRUCTURES OF NEURAL NETWORKS

Network name	Net 1	Net 2	Net 3	Net 4	Net 5	Net 6
Q_r Structure	[N-N-N]	[N-N-N]	[N-N-N]	[N-N]	[N-N]	[N-N]
Q_p Structure	[N-N]	[N-N]	[N-N]	[N]	[N]	[N]
Neuron per layer	10	20	30	10	20	30
Mean Absolute Error (mm)	0.0210	0.0230	0.0263	0.4873	0.1578	0.0847
Max Absolute Error (mm)	0.3154	2.5041	4.4606	5.0075	2.4942	17.2099
Percentage of errors greater than 0.1 mm	1.36	2.12	2.64	85.07	47.85	26.41

Figs. 6a and 6b show postures of the mechanism in the swing and stance phases of the gait cycle, respectively. Fig. 6c shows the values of $\boldsymbol{t}$. Fig. 6d shows the values of $\dot{\boldsymbol{t}}$, it can be observed that velocities at the beginning and end of the phases are equal to zero. Fig. 7 shows the solution of the inverse kinematics using the neural network model. Figs. 7a and 7b shows the values of joint variables q_r and q_p, respectively, and their derivatives. The maximum and minimum values of the rotational joint are $q_{r\max} = 85.53$ deg and $q_{r\min} = 32.81$ deg. The maximum and minimum values of the prismatic joint are $q_{p\max} = 32.14$ mm and $q_{p\min} = 5.59$ mm. The maximum joint velocities for this trajectory are $\dot{q}_{r\max} = 4.46$ rad/s and $\dot{q}_{p\max} = 104.81$ mm/s. The implemented system successfully performed the commanded task. To validate the inverse kinematics, a dynamic multibody simulation was carried out and compared with the MATLAB-based model. For this purpose, a cycle was executed in which the wheel opens and closes, as illustrated in Fig. 6. The validation results are presented in Fig. 8. Along the X-axis, both the simulation and the model exhibit identical behavior, with only a 1 mm deviation in elevation. Along the Y-axis, starting at 2.5 s, minor disturbances appear in the simulation relative to the model, but these are negligible. The values for Q_r and Q_p show identical behavior in both approaches, as evidenced by the graphs.

Figs. 6a and 6b show postures of the mechanism in the swing and stance phases of the gait cycle, respectively. Fig. 6c shows the values of $\boldsymbol{t}$. Fig. 6d shows the values of $\dot{\boldsymbol{t}}$, it can be observed that velocities at the beginning and end of the phases are equal to zero.

Fig. 9 shows three postures of the prototype when performing the programmed trajectory. The implemented system achieved an average execution time of 20 ms per cycle using the neural network-based inverse kinematics model. This execution time resulted in trajectory tracking performance that we consider acceptable. Given the geometrical parameters of the prototype the maximum extension that can be reached by the tip of the foot link is 227.27 mm, that is 51.52 % more than the radius of the mechanism in wheel mode. It is considered that it is necessary to perform a dimensional synthesis study to determine the geometrical parameters that maximize the extension that can be reached by the foot link and thus a greater benefit can be obtained from the mechanism during its operation in leg mode, such as the ability to overcome larger obstacles.

V. CONCLUSION

Mobile robotics has become one of the most promising areas of modern engineering. This paper introduced the design of a novel leg-wheel transformable mechanism. The purpose of this mechanism is to combine the efficiency of wheeled locomotion with the adaptability and terrain-negotiation capabilities of legged systems, fostering innovation in mobile robotics and supporting the advancement of resilient and intelligent infrastructure, in alignment with SDG 9. This work presents several features that make it novel. For example, both actuators must be placed on the chassis, reducing the weight of the wheel and making the mechanism lightweight, unlike other designs proposed in the literature. The presented device has the advantage that the rotation and extension movements of the leg are decoupled, allowing that in wheel mode only one actuator is necessary. In other designs the operation and coordination of all actuators is required to achieve the circular shape in wheel mode. An interesting application of the presented mechanism is the construction of a vehicle with multiple legs of one degree of freedom, where the transformation of all mechanisms is generated by a single actuator.

Given the complexity of solving the inverse kinematics analytically, in this paper two different numerical methods to address this problem were evaluated. In the analysis of the performance of the Newton-Raphson method, it was observed that this technique can diverge or converge to an incorrect solution depending on the initial value of the variable to be solved. In addition, the number of iterations required to reach a solution is unpredictable. Therefore, this method, in this case, is not suitable for on-line calculations to solve inverse kinematics. The second approach was to develop an ANN model. In this work multi-layer perceptron networks were used. A supervised learning approach was employed, where the network is trained with inputs and outputs from a dataset generated using the direct kinematics. The selected network structure was tested with a dataset composed of 10000 points and only 1.3 % of errors were greater than 0.1 mm. The neural network model was implemented in a prototype and its execution time resulted in satisfactory performance in trajectory tracking. The comparison shows that the Newton-Raphson method, despite requiring on average 185 iterations, does not achieve the desired kinematic solution, whereas the neural network provides an accurate result in about 20 ms, highlighting its efficiency and reliability.

The integration of leg-wheel transformable mechanisms can be useful in robots that must adapt to different types of terrain. One example is a robot for domestic applications, where the mobile robot can operate in wheel mode while performing a vacuuming task, and switch to leg mode when it needs to climb a step or ladder, allowing it to continue its task in another area. This type of assistive technology also supports the objectives

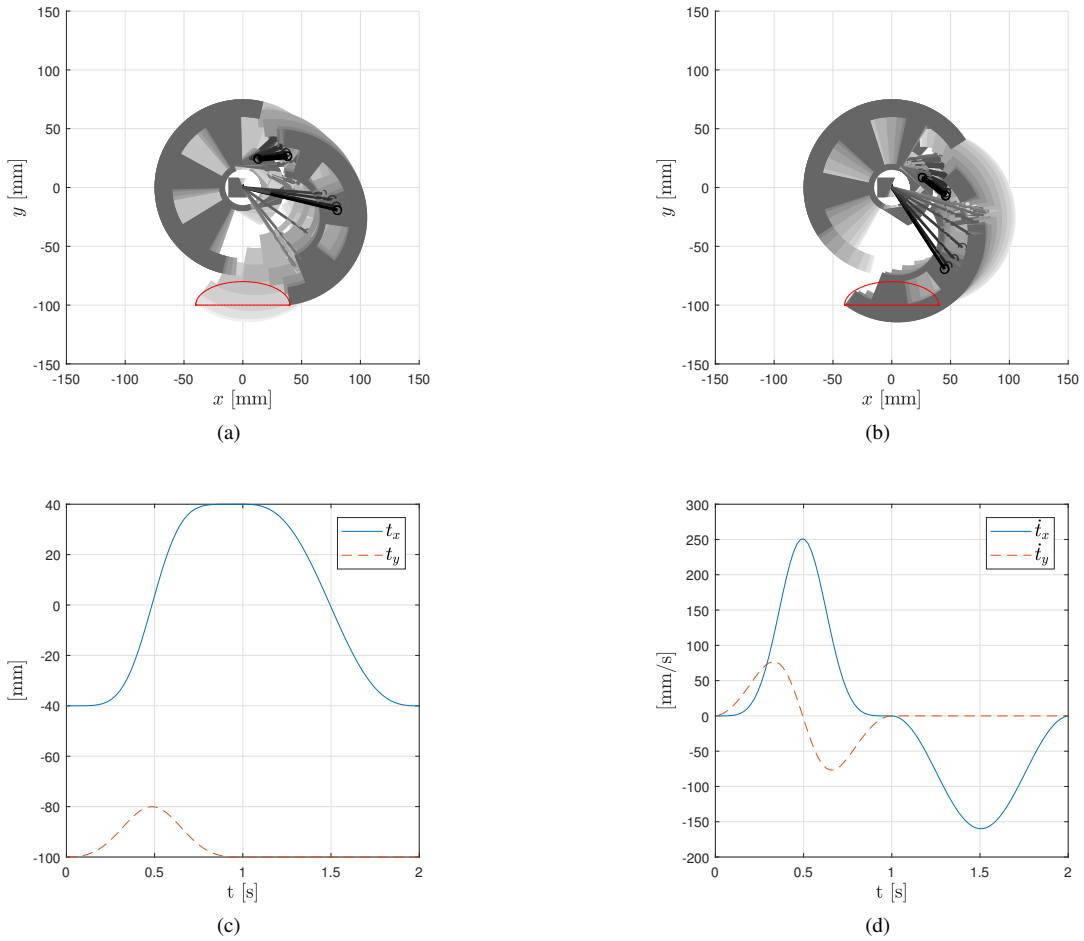

Fig. 6. Trajectory of the gait cycle of the mechanism: a) postures of the mechanism in the swing phase, b) postures of the mechanism in the stance phase, c) positions of the tip the foot link and d) velocities of the tip the foot link.

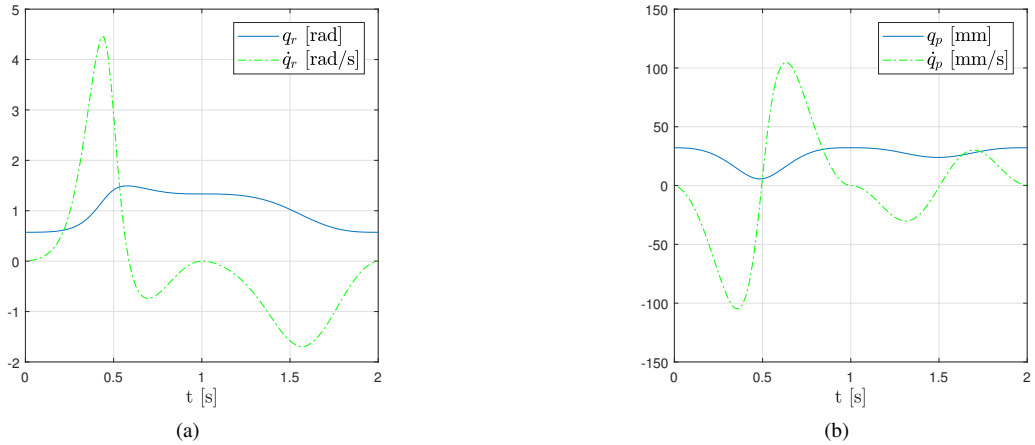

Fig. 7. Solution of the inverse kinematics using the neural network model: a) angular positions and velocities of the rotational joint, b) linear positions and velocities of the prismatic joint.

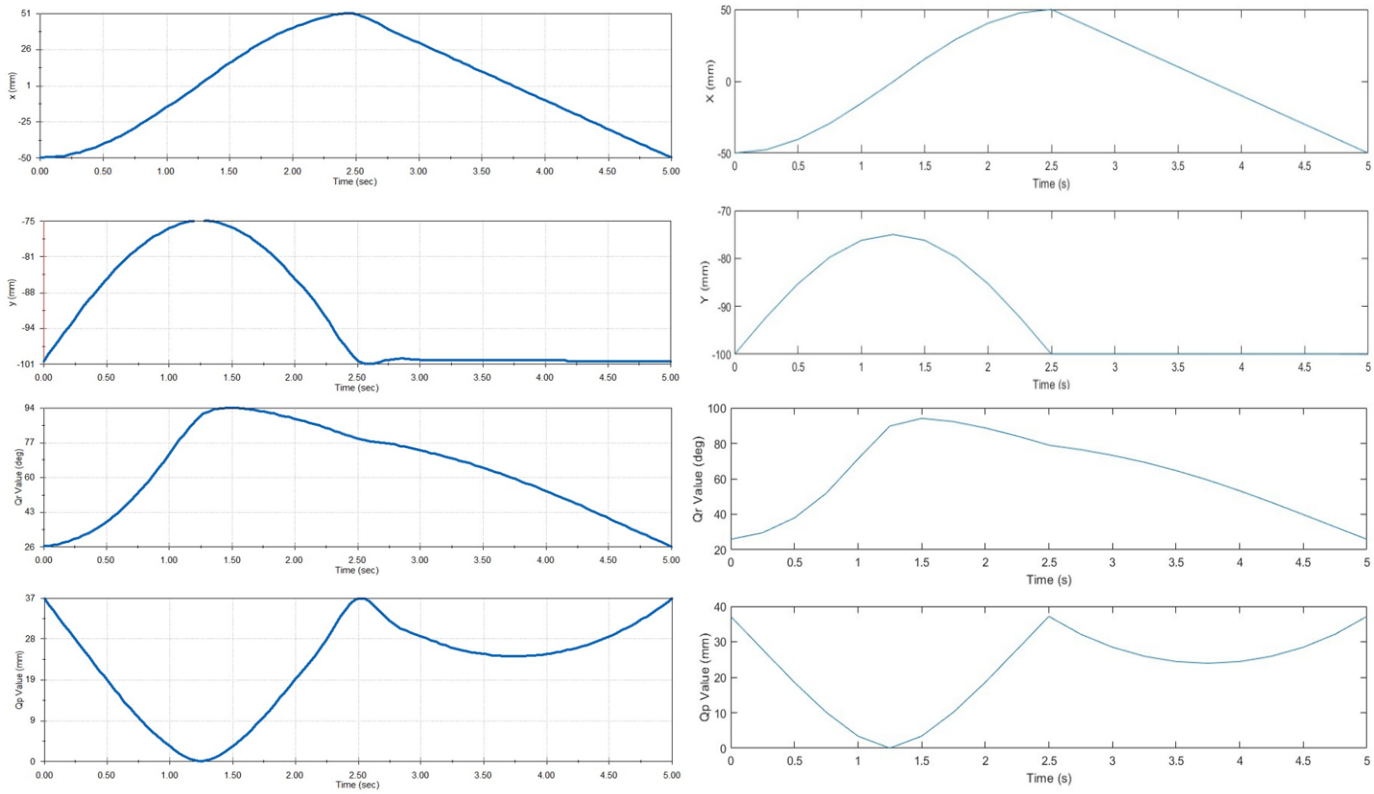

(a) (b)

Fig. 8. Inverse Kinematic validation a) CAD simulation b) Matlab model.

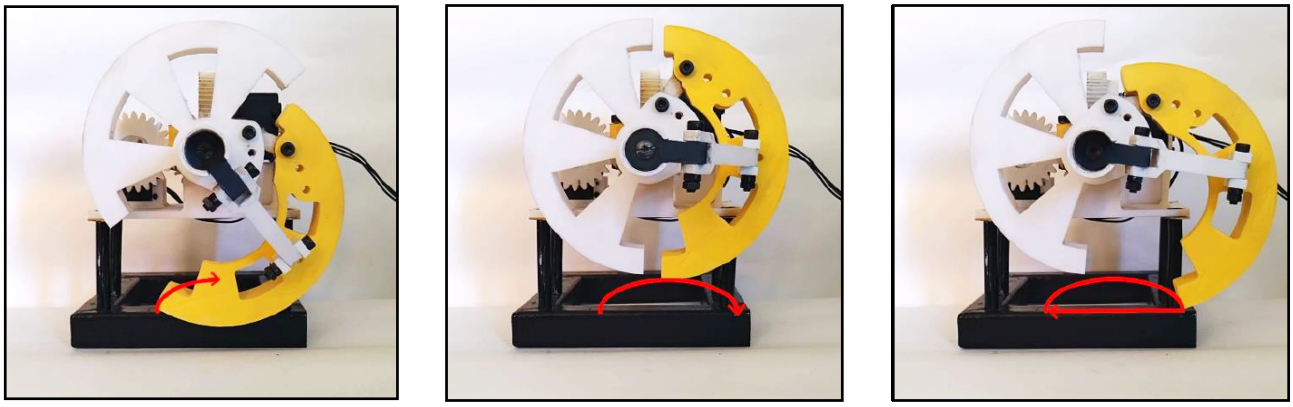

(a) (b) (c)

Fig. 9. Prototype in three positions during the execution of the gait cycle: a) posture at the beginning of the swing phase and at the end of the stance phase, b) posture at the midpoint of the swing phase and c) posture at the end of the swing phase and at the beginning of the stance phase.

of SDG 3 by improving the autonomy and quality of life for individuals with reduced mobility through potential future applications in personal care robotics. Another example is agricultural robots, which when operating in the field can move efficiently in wheel mode in flat areas, but when in plowed or cultivated soils, or in areas where the consistency of the ground changes due to environmental factors (such as mud produced by rainfall), legged locomotion is more appropriate. Such innovations in agricultural automation promote productivity and economic growth, contributing to SDG 8 by supporting the development of efficient and resilient farming practices. Finally, another application is spatial exploration, where there is a variety of terrain, from firm, rocky terrain to dunes, which combine a terrain that is not firm and sloping.

Future work includes optimizing the mechanism's dimensions to extend the foot link and building a prototype for experimental evaluation. Scalability will also be explored by assessing performance in a multi-legged robot such as a hexapod, while addressing potential limitations of the sliding joint in real environments where friction or obstacles may hinder its motion.

REFERENCES

[1] L. Bruzzone and G. Quaglia, "Review article: locomotion systems for ground mobile robots in unstructured environments," *Mechanical Sciences*, vol. 3, pp. 49–62, 07 2012, doi: https://doi.org/10.5194/ms-3-49-2012.

[2] R. Siegwart, I. Nourbakhsh, and D. Scaramuzza, *Introduction to Autonomous Mobile Robots 2nd Edition*. MIT Press, 2011, iSBN: 9780262295093.

[3] D. Lu, E. Dong, C. Liu, M. Xu, and J. Yang, "Design and development of a leg-wheel hybrid robot "hytro-i"," in *2013 IEEE/RSJ International Conference on Intelligent Robots and Systems*, 2013, pp. 6031–6036, doi: https://doi.org/10.1109/IROS.2013.6697232.

[4] G. Qiao, G. Song, Y. Zhang, J. Zhang, and Z. Li, "A wheel-legged robot with active waist joint: Design, analysis, and experimental result," *Journal of Intelligent and Robotic Systems*, vol. 83, pp. 485–502, 2016, dOI: https://doi.org/10.1007/s10846-015-0303-2.

[5] R. Siegwart, P. Lamon, T. Estier, L. Lauria, and R. Piguet, "Innovative design for wheeled locomotion in rough terrain," *Robotics and Autonomous Systems.ISSN 0921-8890*, vol. 40, pp. 151–162, 2002, doi: https://doi.org/10.1016/S0921-8890(02)00240-3.

[6] F. Cordes, A. Dettmann, and F. Kirchner, "Locomotion modes for a hybrid wheeled-leg planetary rover," in *2011 IEEE International Conference on Robotics and Biomimetics*, 2011, pp. 2586–2592, dOI: https://doi.org/10.1109/ROBIO.2011.6181694.

[7] R. Quinn, J. Offi, D. Kingsley, and R. Ritzmann, "Improved mobility through abstracted biological principles," vol. 3, 02 2002, pp. 2652 – 2657 vol.3, doi: https://doi.org/10.1109/IRDS.2002.1041670.

[8] M. Eich, F. Grimminger, and F. Kirchner, "A versatile stair-climbing robot for search and rescue applications," in *2008 IEEE International Workshop on Safety, Security and Rescue Robotics*, 2008, pp. 35–40, doi: https://doi.org/10.1109/SSRR.2008.4745874.

[9] J. L. Ordoñez-Avila, H. A. Moreno, M. E. Perdomo, and I. G. C. Calderón, "Designing legged wheels for stair climbing," *Symmetry*, vol. 15, no. 11, 2023, doi: https://doi.org/10.3390/sym15112071.

[10] I. T. Burt and N. P. Papanikolopoulos, "Adjustable diameter wheel assembly, and methods and vehicles using same," US 6860346, 2005.

[11] Y. Lin, H. Lin, and P. Lin, "Slip-model-based dynamic gait generation in a leg-wheel transformable robot with force control," *IEEE Robotics and Automation Letters*, vol. 2, no. 2, pp. 804–810, April 2017, doi: https://doi.org/10.1109/LRA.2017.2653363.

[12] H. Moreno, I. Carrera, J. P. García, and J.Baca, "Heise wheels: a family of mechanisms for implementing variable geometry hybrid wheels," *Revista Iberoamericana de Automática e Informática industrial*, vol. 15, no. 4, 2018, dOI: https://doi.org/10.4995/riai.2017.8798.

[13] K. Tadakuma, R. Tadakuma, A. Maruyama, E. Rohmer, K. Nagatani, K. Yoshida, A. Ming, M. Shimojo, M. Higashimori, and M. Kaneko, "Mechanical design of the wheel-leg hybrid mobile robot to realize a large wheel diameter," in *2010 IEEE/RSJ International Conference on Intelligent Robots and Systems*, Oct 2010, pp. 3358–3365, dOI: https://doi.org/10.1109/IROS.2010.5651912.

[14] P. Lin and S. Shen, "Mobile platform," US 8307923 B2, 2012.

[15] H.-Y. Chen, T.-H. Wang, K.-C. Ho, C.-Y. Ko, P.-C. Lin, and P.-C. Lin, "Development of a novel leg-wheel module with fast transformation and leaping capability," *Mechanism and Machine Theory*, vol. 163, p. 104348, 2021, doi: https://doi.org/10.1016/j.mechmachtheory.2021.104348.

[16] Y. Xue, X. Yuan, Y. Wang, Y. Yang, S. Lu, B. Zhang, J. Lai, J. Wang, and X. Xiao, "Lywal: a leg-wheel transformable quadruped robot with picking up and transport functions," 05 2021, pp. 2935–2941, doi: https://doi.org/10.1109/ICRA48506.2021.9561128.

[17] H. A. Moreno, "Kinematic analysis of a novel leg-wheel transformable mechanism," in *Advances in Automation and Robotics Research*, M. N. Cardona, J. Baca, C. Garcia, I. G. Carrera, and C. Martinez, Eds. Cham: Springer Nature Switzerland, 2024, pp. 46–55, doi: https://doi.org/10.1007/978-3-031-54763-8_5.

[18] Y. Li, Z. Wei, J. Guo, J. Ren, Y. Ding, W. Wang, J. Liu, and A. Song, "A stair-climbing wheelchair with novel spoke wheels for smooth motion," *Applied Sciences*, vol. 15, no. 10, 2025. [Online]. Available: https://www.mdpi.com/2076-3417/15/10/5433

[19] J. L. Ordonez Avila and J. Fernandez-Olivares, "A Mobile Robot with Deep Learning for Monitoring Coffee Farms," in *Proceedings of the 22nd LACCEI International Multi-Conference for Engineering, Education and Technology (LACCEI 2024): "Sustainable Engineering for a Diverse, Equitable, and Inclusive Future at the Service of Education, Research, and Industry for a Society 5.0."*. Latin American and Caribbean Consortium of Engineering Institutions, 2024. [Online]. Available: https://laccei.org/LACCEI2024-CostaRica/meta/FP1924.html

[20] R. A. et al., "Rhex: A biologically inspired hexapod runner," *Auton. Robots*, vol. 11, no. 2, pp. 207–2013, 2001, doi: https://doi.org/10.1023/A:1012426720699.

[21] L. Puglisi, R. Saltaren, C. Garcia Cena, P.-F. Cardenas, and H. Moreno Avalos, "Implementation of a generic constraint function to solve the direct kinematics of parallel manipulators using newton-raphson approach," *Control Engineering and Applied Informatics*, vol. 19, pp. 71–79, 01 2017.

[22] A.-V. Duka, "Neural network based inverse kinematics solution for trajectory tracking of a robotic arm," 2014, dOI: https://doi.org/10.1016/j.protcy.2013.12.451.

[23] H. Sadjadian and H. Taghirad, "Comparison of different methods for computing the forward kinematics of a redundant parallel manipulator," *Journal of Intelligent and Robotic Systems*, vol. 44, pp. 225–246, 11 2005, doi: https://doi.org/10.1007/s10846-005-9006-4.

[24] A. Zubizarreta, M. Larrea, E. Irigoyen, I. Cabanes, and E. Portillo, "Real time direct kinematic problem computation of the 3prs robot using neural networks," *Neurocomputing*, vol. 271, pp. 104–114, 2018, doi: https://doi.org/10.1016/j.neucom.2017.02.098.

[25] J. F. Flores, H. A. Moreno, I. G. Carrera, M. A. Garcia, and R. G. Adan, "Inverse kinematics of a rsrr heise wheel using neural networks," in *2021 XXIII Robotics Mexican Congress (ComRob)*, 2021, pp. 19–24, doi: https://doi.org/10.1109/ComRob53312.2021.9628728.

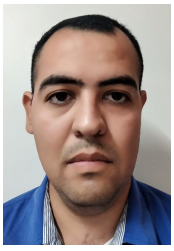

José F. Flores holds a B.S. in Industrial Electronics Engineering and an M.Sc. in Electrical Engineering from Universidad Autónoma de Coahuila, Mexico (2017, 2021). He has industrial experience as engineer, and has been teaching at different institution such as the UPIIC of the Instituto Politécnico Nacional. His research interest are in the fields of robotics, AI, manufacturing and industrial automation.

Héctor A. Moreno holds a M.Sc. and Ph.D. in Automation and Robotics from Universidad Politécnica de Madrid (2009, 2013). He holds a B.S. in Mechanical Engineering and an M.Sc. in Electrical Engineering from Instituto Tecnológico de la Laguna, Mexico (2004, 2006). With extensive experience as a professor and researcher at various Mexican universities, he has also taught graduate courses across Latin America and visited research institutes in France, Japan, and the U.S. He has authored over 60 publications and edited four books. Currently a Research Professor at Universidad Autónoma de Coahuila, his research focuses on modeling, control, and design of field, service, and industrial robots.

Isela G. Carrera holds a Ph.D. in Automation and Robotics from Universidad Politécnica de Madrid (2013). She holds a B.S. in Electronic and Telecommunications Engineering from ITESM Monterrey and an M.S. in Electrical Engineering from Instituto Tecnológico de la Laguna. In 2017, she became a member of Mexico's National System of Researchers. Dr. Carrera has published over 30 papers, book chapters, and edited 4 books. She is currently a Research Professor at Universidad Autónoma de Coahuila, focusing on the design of multifunctional rehabilitation devices for lower limb disabilities.

José Luis Ordoñez Ávila holds multiple degrees: a B.Eng. in Electronic Engineering (2015), a B.Eng. in Industrial Engineering (2008), an M.S. in Project Administration (2017), an M.S. in Industrial Engineering (2020), an M.S. in Engineering for Industry with Robotics (2023), and a Doctorate in Business Administration (2024). He is a tenured professor at UNITEC, specializing in robotics, mechatronics, and research. Dr. Ordoñez has taught at Universidad Tecnológica de El Salvador and been a researcher at Universidad Evangélica de El Salvador. His research focuses on robotics, AI, control systems and industrial automation.